# LARGE-SCALE THERMAL ANALYSIS OF COMPOSITES EMBEDDED WITH CNTS OF ARBITRARY SHAPES AND RANDOM DISTRIBUTION

Masataka TANAKA [1)], Jianming ZHANG [2)]

1) Faculty of Engineering, Shinshu University, (Nagano 380-8553,     E-mail: dtanaka@gipwc.shinshu-u.ac.jp)

2) Faculty of Engineering, Shinshu University, (Nagano 380-8553,     E-mail: zhangjm@homer.shinshu-u.ac.jp)

The superior thermal conductivity of carbon nanotube (CNT) makes the material promising in development of fundamentally new composites. To study the influence of CNTs distribution on the overall properties of the composite, modeling of a Representative Volume Element (RVE) including a large number of CNTs that are randomly distributed and oriented is necessary. However, analysis of such an RVE using standard numerical methods faces two severe difficulties: discretization of the geometry and the very large computational scale. In this paper, the first difficulty is alleviated by employing the Hybrid Boundary Node Method (HdBNM). To overcome the second difficulty, a simplified mathematical model is proposed to reduce the total degrees of freedom of the problem by nearly half. Then, the Fast Multipole Method (FMM) is combined with the HdBNM based on the simplified model to further reduce the computational scale, resulting in an efficient tool for large-scale simulation. The developed code is employed to compute the equivalent heat conductivities of RVEs containing various numbers of CNTs with different lengths, shapes and alignments. Insights have been gained into the thermal behavior of the composite material.

*Keywords*: hybrid boundary node method, CNT-based composites, fast multipole method, heat conduction

## 1. Introduction

In recent years, intensive research has been carried out on carbon nanotubes (CNT) concerning their production, physical properties and possible applications [1, 2]. Due to their near-perfect nanostructure, the carbon nanotubes (CNT) possess exceptional physical properties such as superior thermal and electrical conductivities, as well as high stiffness and strength. These remarkable properties may make CNTs ideal for a wide range of technological applications. One of the most intriguing applications is the use of CNTs, as small volume fraction filler, in nanotube-reinforced polymers. CNT-based composites offer significant improvements to structural properties over their base polymers. It has been demonstrated that with only 1% (weight fraction) of CNTs added to a matrix material, the stiffness of a resulting composite can increase as high as 36%-42% and the tensile strength up to 25% [3]. In the work of Biercuk et al. [4], samples of industrial epoxy loaded with 1 wt% single-walled CNTs showed a 70% increase in heat conductivity at 40K, and rose to 125% at room temperature.

Numerical simulations can help to understand of the relationship between the geometrical characteristic (e.g. nanotube orientation) and the properties of the nanocomposites. This will allow the determination and optimization of different processing method to manufacture the nanocomposite materials. At the nanoscale level, atomistic or molecular dynamics (MD) have been somehow "natural" simulation methods, and have provided abundant results helping in understanding their thermal, mechanical and electrical behaviors [5]. However, due to the limitations in current computing power, these simulations are so far limited to single individual pure CNTs or very small scales for CNT-composite; for example, an RVE including single short CNT, only. To study the influence of CNT's distribution on the equivalent properties of the composite, modeling of an RVE including a large number of CNTs that are randomly distributed and oriented is necessary. This is because, in a real CNT-composite, the CNTs are not uniform in size and shape. They can be straight, twisted and curled or in the form of ropes and their distribution and orientation in the matrix can be nonuniform, unidirectional or random. Even with the most superior computer resources available in the world, computation of such an RVE by MD is almost impossible. Liu et al. [6] has demonstrated that the use of atomistic or molecular dynamics (MD) simulations is inevitable for the analysis of such nanomaterials in order to study the local load transfers, interface properties, or failure modes at the nanoscale. However, for the global analysis studying the effects of CNTs configuration on the overall properties of the material, they suggested a continuum model, in which the physical behavior of the composite is governed by continuum equations such as Laplace's equation for thermal property and Lame-Navier equations for elastic properties.

This study aims at gaining insight into the thermal properties of CNT-based composites through numerical simulation. The equivalent heat conductivity of carbon nanotube-based composites is evaluated using a

representative volume element (RVE) based on 3-D potential theory.

For the analysis of an RVE in which not only single but many CNTs are randomly distributed, the implementation of standard numerical solution techniques like FEM or BEM may face severe difficulties in discretization of the domain geometry in question. This is valid especially for FEM models where meshing of the solid geometries within CNT-reinforced polymers may be tedious and extremely difficult. To alleviate this difficulty the hybrid boundary node method (HdBNM) can be used [7, 8]. By combining a modified functional with the moving least squares (MLS) approximation, the HdBNM is a truly meshless, boundary-only method. We have combined the HdBNM with a multi-domain solver and applied the combined approach to perform some preliminary computations and investigate the influences of the CNT length, curvature and dispersion on the equivalent thermal properties of the composites [9, 10].

However, these computations are limited to relatively small scales, as usually only single or several but shorter CNTs were considered. Due to the very thin and slender structure of the CNTs, a large number of nodes are required to discretize them in order to capture the steep gradients. Moreover, in a multi-domain solver, at each node on the interface of a CNT with the host polymer, both temperature and normal flux are unknown. This situation considerably increases the total degrees of freedom in the overall system of equations.

The preliminary studies have also shown that temperatures within the entire CNT are almost uniform due to the huge difference of heat conductivity between the CNT and the host polymer. Based on this observation, we have proposed a simplified mathematical model, where the CNTs are considered as heat superconductors and uniform temperature distributions within the entire body of each CNT assumed [11]. As a result, the total number of degrees of freedom is reduced by nearly half, and thus increases the number of CNTs contained in an RVE that can be analyzed within available computer resources. The simplified model has been rigorously tested and validated using benchmark examples.

Nevertheless, even with the simplified model, both the memory requirements and the computational scale are still of $O(N^2)$, (when an iterative solver applied, if a direct solver, the Gauss elimination for example, is used, the computational scale is even higher up to $O(N^3)$)), where $N$ stands for the total number of degrees of freedom. To perform analysis of a real-world RVE model, an efficient technique further reducing computational requirements is necessary. The method of choice is FMM.

The FMM was introduced by Rokhlin [12], and developed by Greengard [13] as an algorithm for the rapid evaluation of Coulombic interactions in a large scale ensemble of particles. In their method, multipole moments are used to represent distant particle groups, a local expansion to evaluate the contribution from distant particles in the form of a series, and a hierarchical decomposition of the domain to carry out efficient and systematic grouping of the particles. The FMM reduces both memory size and computational scale from $O(N^2)$ to $O(N)$, thus enabling scientific and engineering computations that were previously impossible.

The FMM has been applied to a variety of computation methods. Applying FMM to accelerate BEM computation has been investigated by many researchers [14, 15]. We have combined the FMM with HdBNM for large scale computation of potential problems [16]. In this paper, the FMM techniques are implemented into the HdBNM based on the simplified model for simulation of thermal behavior of CNT-based composites. RVEs containing a number of CNTs with different lengths, shapes and alignments, have been studied. It is realized that some specific alignments may significantly increase the equivalent heat conductivity of the composites.

## 2. Simplified mathematical model for CNT composites

As mentioned in the introduction, the unusually high heat conductivity of the CNTs in comparison with the polymer makes the temperature distribution within an individual CNT almost uniform. This feature allows us to simplify the modeling of the CNT-based composites. In this section the formulations for the simplified mathematical model are developed, where only single domain, namely the polymer matrix is modeled. Each CNT is treated as a heat superconductor with one constant temperature constrained at its surface. A similar assumption can be found in a rigid-line inclusion model [17].

Suppose that $n$ CNTs are distributed in a polymer matrix which makes an RVE. It is assumed that the matrix is continua of linear, isotropic and homogenous materials with given heat conductivities. A steady state heat conduction problem governed by Laplace's equation with proper boundary conditions is considered.

The HdBNM is based on a modified variational principle, in which there are three independent variables, namely:
- temperature within the domain, $\phi$;
- boundary temperature, $\tilde{\phi}$;
- boundary normal heat flux, $\tilde{q}$.

Suppose further that $N$ nodes are randomly distributed on the surfaces (including the interfaces with CNTs) of the polymer domain. The temperature within the domain is approximated using fundamental solutions as follows:

$$\phi = \sum_{J=1}^{N} \phi_J^s x_J \qquad (1)$$

and hence the normal heat flux is given by:

$$q = -\kappa \sum_{J=1}^{N} \frac{\partial \phi_J^s}{\partial n} x_J \qquad (2)$$

where $\phi_J^s$ is the fundamental solution with the source at a node $\mathbf{s}_J$, $\kappa$ is the heat conductivity and $x_J$ are unknown parameters. For 3-D steady state heat conduction problems, the fundamental solution can be written as

$$\phi_J^s = \frac{1}{\kappa} \frac{1}{4\pi r(Q, \mathbf{s}_J)} \qquad (3)$$

where $Q$ is a field point; $r(Q, \mathbf{s}_J)$ is the distance between $Q$ and $\mathbf{s}_J$.

The boundary temperature and normal heat flux are approximated by moving least square (MLS) approximation:

$$\tilde{\phi}(\mathbf{s}) = \sum_{J=1}^{N} \Phi_J(\mathbf{s})\hat{\phi}_J \qquad (4)$$

and

$$\tilde{q}(\mathbf{s}) = \sum_{J=1}^{N} \Phi_J(\mathbf{s})\hat{q}_J \qquad (5)$$

In the foregoing equations, $\Phi_J(\mathbf{s})$ is the shape function of MLS approximation; $\hat{\phi}_J$ and $\hat{q}_J$ are nodal values of temperature and normal flux, respectively.

For the polymer domain, the following set of HdBNM equations can be written:

$$\begin{bmatrix} U_{00} & U_{01} & \cdots & U_{0n} \\ U_{10} & U_{11} & \cdots & U_{1n} \\ \vdots & \vdots & \ddots & \vdots \\ U_{n0} & U_{n1} & \cdots & U_{nn} \end{bmatrix} \begin{Bmatrix} x_0 \\ x_1 \\ \vdots \\ x_n \end{Bmatrix} = \begin{Bmatrix} H_0\hat{\phi}_0 \\ H_1\hat{\phi}_1 \\ \vdots \\ H_n\hat{\phi}_n \end{Bmatrix} \qquad (6)$$

$$\begin{bmatrix} V_{00} & V_{01} & \cdots & V_{0n} \\ V_{10} & V_{11} & \cdots & V_{1n} \\ \vdots & \vdots & \ddots & \vdots \\ V_{n0} & V_{n1} & \cdots & V_{nn} \end{bmatrix} \begin{Bmatrix} x_0 \\ x_1 \\ \vdots \\ x_n \end{Bmatrix} = \begin{Bmatrix} H_0\hat{q}_0 \\ H_1\hat{q}_1 \\ \vdots \\ H_n\hat{q}_n \end{Bmatrix} \qquad (7)$$

where subscripts 0 and $k\,(=1,\cdots,n)$, stand for quantities exclusively associated with the polymer domain, and quantities associated with its interface with the $k$-th nanotube, respectively. The sub-matrices $[U]$, $[V]$ and $[H]$ are given as:

$$U_{IJ} = \int_{\Gamma_I} \phi_J^s v_I(Q)\,d\Gamma \qquad (8)$$

$$V_{IJ} = -\kappa \int_{\Gamma_I} \frac{\partial \phi_J^s}{\partial n} v_I(Q)\,d\Gamma \qquad (9)$$

$$H_{IJ} = \int_{\Gamma_I} \Phi_J(\mathbf{s})v_I(Q)\,d\Gamma \qquad (10)$$

where $\Gamma_I$ is a regularly shaped local region around a collocation node $\mathbf{s}_I$, $v_I$ is a weight function and $\mathbf{s}$ is a field point on the boundary. For full details of HdBNM refer to [8].

By combining Eqs. (6) and (7), we have the following equation:

$$\begin{bmatrix} A_{00} & A_{01} & \cdots & A_{0n} \\ U_{10} & U_{11} & \cdots & U_{1n} \\ \vdots & \vdots & \ddots & \vdots \\ U_{n0} & U_{n1} & \cdots & U_{nn} \end{bmatrix} \begin{Bmatrix} x_0 \\ x_1 \\ \vdots \\ x_n \end{Bmatrix} = \begin{Bmatrix} H_0 d_0 \\ H_1\hat{\phi}_1 \\ \vdots \\ H_n\hat{\phi}_n \end{Bmatrix} \qquad (11)$$

where, each row of sub-matrices $\left[A_{0k}\right], k = 0,1,\cdots,n$, is supplied identically from that in $\left[U_{0k}\right]$ or $\left[V_{0k}\right]$ according to the boundary condition at the corresponding node, and the corresponding term of $\{d_0\}$ comes from $\{\hat{\phi}_0\}$ or $\{\hat{q}_0\}$.

Further suppose that $m_k$ nodes are located at the interface of $k$-th nanotube with the polymer, and a constant

temperature $\phi_c^k$ is prescribed, namely

$$\left\{\hat{\phi}_k\right\} = \{\mathbf{1}\}_k\,\phi_c^k \qquad (12)$$

where $\left\{\hat{\phi}_k\right\}$ are the nodal values of temperature at the interface; $\{\mathbf{1}\}_k$ is a column vector of $m_k$ dimensions with all the elements equal 1. Inserting Eq. (12) into Eq. (11) for all interfaces, the following equation is obtained,

$$\begin{bmatrix} A_{00} & A_{01} & \cdots & A_{0n} & 0 & \cdots & 0 \\ U_{10} & U_{11} & \cdots & U_{1n} & -H_1\{\mathbf{1}\}_1 & \cdots & 0 \\ \vdots & \vdots & \ddots & \vdots & \vdots & \ddots & \vdots \\ U_{n0} & U_{n1} & \cdots & U_{nn} & 0 & \cdots & -H_n\{\mathbf{1}\}_n \end{bmatrix} \begin{Bmatrix} x_0 \\ x_1 \\ \vdots \\ x_n \\ \phi_c^1 \\ \vdots \\ \phi_c^n \end{Bmatrix} = \begin{Bmatrix} H_0 d_0 \\ 0 \\ \vdots \\ 0 \end{Bmatrix} \qquad (13)$$

In the above set of equations, there are $n$ (the number of CNTs) more unknowns than the number of equations, because we have introduced one additional unknown, i.e. the constant temperature, for each CNT. In order to solve Eq. (13), we have to add $n$ extra equations. These equations can be obtained from energy conservation law. Actually, in steady state heat conduction, the rate of thermal energy flowing into a CNT must equal that flowing out. Therefore, the following relationship exists at the surface of the $k$-th CNT,

$$\int_{C_k} q\,d\Gamma = 0 \qquad (14)$$

where $C_k$ represents the outer surface of the $k$-th CNT. Substituting Eq. (2) into (14) and omitting the common factor $\kappa$, we have

$$\sum_{J=1}^{N} \int_{C_k} \frac{\partial \phi_J^s}{\partial n}\,d\Gamma\, x_J = 0 \qquad (15)$$

In Eq. (15), $C_k$ is a closed surface. The following integral identity holds [18],

$$\int_{C_k} \frac{\partial \phi_J^s}{\partial n}\,d\Gamma = \begin{cases} 1, & \forall \mathbf{s}_J \in C_k \\ 0, & \forall \mathbf{s}_J \notin C_k \end{cases} \qquad (21)$$

Therefore, the coefficients in Eq. (15) are either 1 or 0. For nodes located on the surface of the $k$-th CNT, they are 1, otherwise they are 0. Appending Eq. (15) to Eq. (13) for all CNTs, we obtain the final set of algebraic equations system which can uniquely determine the unknown parameter $x$.

$$\begin{bmatrix} A_{00} & A_{01} & \cdots & A_{0n} & 0 & \cdots & 0 \\ U_{10} & U_{11} & \cdots & U_{1n} & -H_1\{\mathbf{1}\}_1 & \cdots & 0 \\ 0 & \{\mathbf{1}\}_1^{\mathrm{T}} & \cdots & 0 & 0 & \cdots & 0 \\ \vdots & \vdots & \ddots & \vdots & \vdots & \ddots & \vdots \\ U_{n0} & U_{n1} & \cdots & U_{nn} & 0 & \cdots & -H_n\{\mathbf{1}\}_n \\ 0 & 0 & \cdots & \{\mathbf{1}\}_n^{\mathrm{T}} & 0 & \cdots & 0 \end{bmatrix} \begin{Bmatrix} x_0 \\ x_1 \\ \vdots \\ x_n \\ \phi_c^1 \\ \vdots \\ \phi_c^n \end{Bmatrix} = \begin{Bmatrix} H_0 d_0 \\ 0 \\ 0 \\ \vdots \\ 0 \\ 0 \end{Bmatrix} \qquad (17)$$

The total number of degrees of freedom in Eq. (17) is

relatively very small when compared with that of a full model (multi-domain solver, see [9]). For each CNT, only one algebraic equation is added. Moreover, as the coefficients of these algebraic equations are either 1 or 0, calculations of them are avoided. Therefore, both the CPU time and memory usage can be saved significantly.

The set of Eq. (17) is solved for the unknown parameters $x$, and then, by back-substitution into Eqs. (6) and (7), the boundary unknowns are obtained either on the interfaces or the external boundary surfaces. As demonstrated, the HdBNM is a boundary-only meshless approach. No boundary elements are used for either interpolation or integration purposes. Therefore, it may alleviate the discretization task to a large extent for complicated geometries.

## 3. Accelerating equation solution by FMM

The size of the coefficient matrix in Eq. (17) is dominated by sub-matrices $\left[ A_{0k} \right]$ and $\left[ U_{ki} \right]$, $k=1,\cdots,n$, $i=0,1,\cdots,n$. Since these sub-matrices are unsymmetrical and fully populated, solving Eq. (17) by an iterative solver requires $O(N^2)$ operations. In this paper, we use the restarted preconditioned GMRES to solve Eq. (17). The most time-consuming aspect of an iterative method when employed for solving a system of linear equations is the matrix-vector product in each iteration step. Taking an iteration vector $\mathbf{x}'$ into account, the product of a row of the coefficient matrix in Eq. (17) and the guess vector $\mathbf{x}'$ can be expressed as one of the following four sums:

$$\sum_{J=1}^{N} \int_{\Gamma_I} \phi_J^s v_I(Q) x_J' d\Gamma \qquad (18)$$

$$\sum_{J=1}^{N} \int_{\Gamma_I} -\kappa \frac{\partial \phi_J^s}{\partial n} v_I(Q) x_J' d\Gamma \qquad (19)$$

$$\sum_{J=1}^{N} \int_{\Gamma_I} \phi_J^s v_I(Q) x_J' d\Gamma + \phi_c^k \sum_{J}^{m_k} H_{IJ} \qquad (20)$$

$$\sum_{J}^{m_k} x_J^k \qquad (21)$$

Sums (18) and (19) are related to a node located on the external boundary and prescribed with temperature and normal flux, respectively. Sum (20) is related to a node located at the interface of the $k$-th CNT with the polymer domain, and Expression (21) to the $k$-th uniform temperature constraint.

The computational costs for the second term in sum (20) and sum (21) are trivial, and can be ignored. The summations (18) and (19) are accelerated by FMM at the cost of $O(N)$. For full details of fast multipole HdBNM refer to [16].

## 4. Study on thermal behavior of CNT-based composites

In this section, we use an RVE to study the CNT-based composites for their thermal properties. The RVE are modeled with straight or curved CNTs embedded, and with properly applied boundary conditions. A rectangular RVE is employed with the dimensions shown in Fig. 1. Based on the simplified mathematical model, the CNTs are treated as cavities which are identical to the outer surfaces of the CNTs. A constant temperature is constrained at a cavity

surface. The radii of CNTs ($R$=5 nm) are kept constant in all the following examples, while their length and shapes, together with the number of CNTs and their alignments, varies for different examples. The heat conductivity, $\kappa^p$, used for the polymer (polycarbonate) is 0.37 W/m·K, and for CNT 1750 W/m·K. Uniform temperatures of 300K and 200K are imposed at the two end faces of the RVE, respectively, and heat flux free at other four side faces. This boundary condition set allows us to estimate equivalent heat conductivity of the composite in the axial direction. Using Fourier's law, the formula for equivalent heat conductivity can be written as

$$\kappa = -\frac{qL}{\Delta\phi} \qquad (35)$$

where $\kappa$ represents the heat conductivity; $q$ is the average value of normal flux at the two end face, obtained by HdBNM; $L$ is the length of the RVE in the axial direction and $\Delta\phi$ the temperature difference between the two end faces.
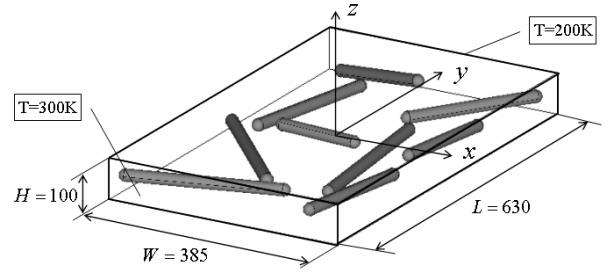


Fig. 1  Dimensions of a Nanoscale RVE.

Computations are performed on a desktop computer with an Intel(R) Pentium(R) 4 CPU (1.99GHz). Following Reference [8], we truncate all the infinite expansions after $p$=10, set the maximum number of boundary nodes in a leaf box to be 60, and terminate the iteration when the relative error is less than $10^{-6}$.

Eight RVEs containing different numbers of CNTs with different shapes, alignments, have been considered. These RVEs are presented in Figs. 2. Results of our experiments are summarized in Tables 1. In the table, the first row indicates the alignment of CNTs. The second and third rows list the equivalent heat conductivity and volume fraction of CNT, respectively. To assess the enhancement effectiveness, we use as the criterion the ratio of the equivalent heat conductivity to the volume percentage of CNT, which is presented in the fourth row of the table.
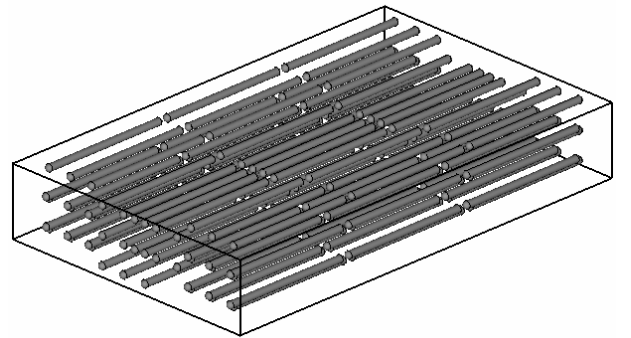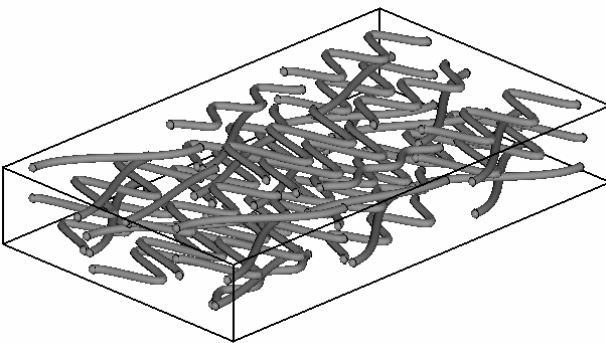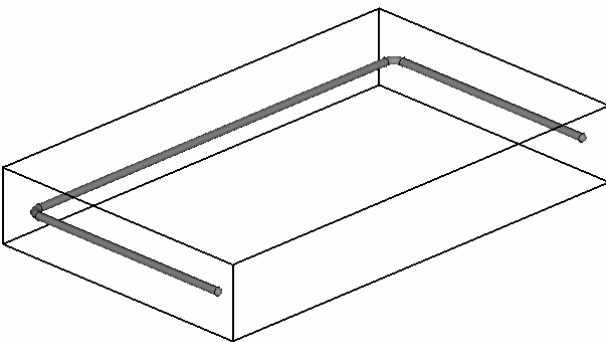


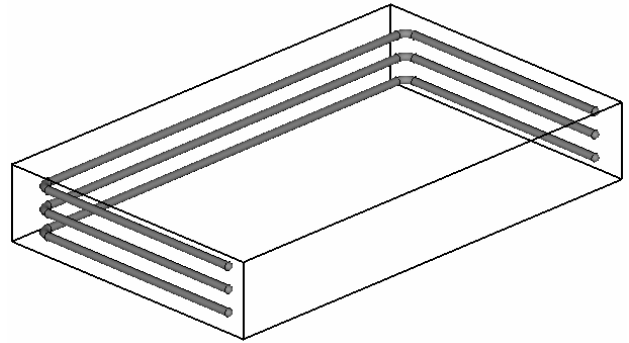(a)  Uniformly located 135 CNTs.
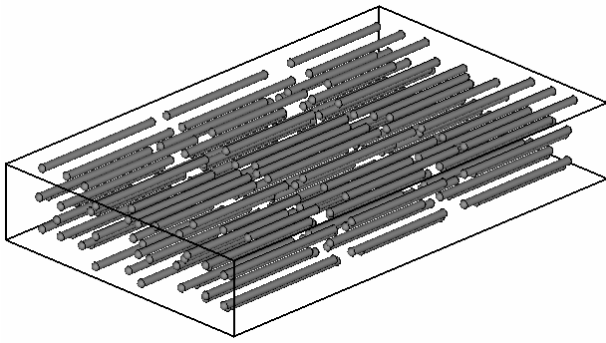
(b) "Randomly" located 135 CNTs.
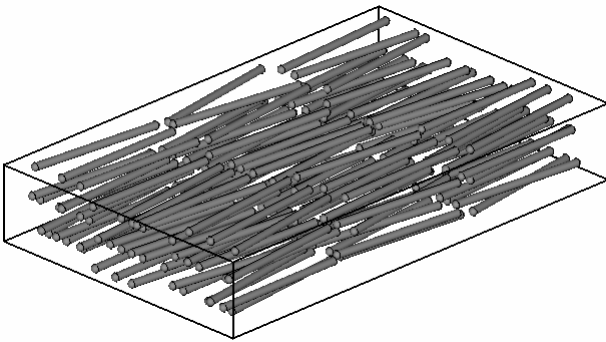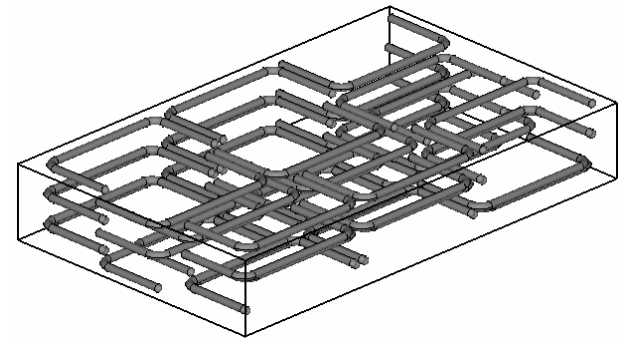

(c) "Randomly" oriented 135 CNTs.


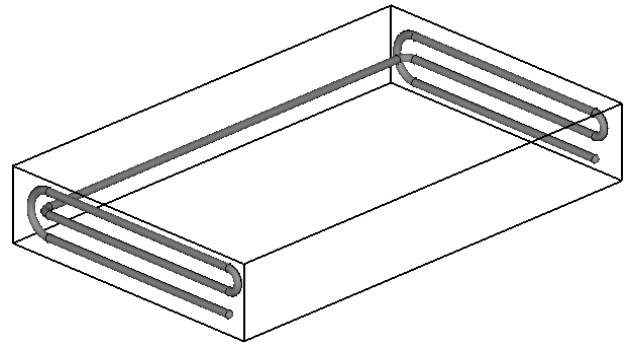(d) "Randomly" located 45 curved CNTs


(e) Single CNT of "C" shape


(f) Three CNTs of "C" shape.


(g) Forty-five CNTs of "C" shape.


(h) Single long and curved CNTs.

Fig. 2 Nanoscale RVEs containing various nanotubes

Table 1. Equivalent heat conductivities for RVEs

| RVE | (a) | (b) | (c) | (d) |
|---|---|---|---|---|
| Conductivity, $\kappa$ (W/m·K) | 3.746 | 2.668 | 3.470 | 1.717 |
| Percentage, $r$ | 8.4% | 7.7% | 8.4% | 4.8% |
| $\kappa/r$ | 44.71 | 35.55 | 41.41 | 36.00 |
| RVE | (e) | (f) | (g) | (h) |
| Conductivity, $\kappa$ (W/m·K) | 4.868 | 11.15 | 6.319 | 11.76 |
| Percentage, $r$ | 0.40% | 1.2% | 5.5% | 0.88% |
| $\kappa/r$ | 1218 | 929.9 | 114.5 | 1337 |

## 5. Concluding remarks

In this paper, formulations of a simplified mathematical model for simulation of thermal behavior of CNT-based composites are presented. The model provides remarkable improvement in computational efficiency. The FMM is employed to further reduce the computational costs.

The proposed approach has been applied to large scale simulation of thermal behavior of CNT composites. From the numerical results, the following conclusions can be made on the influence of CNT length, shape and configuration on the thermal properties of the composite:

1. Comparison among results for cases (a), (b), (c) and (d) shows that the CNT distribution, orientation and waviness affect the equivalent heat conductivity, but their influences on the ratio $\kappa/r$ are not strong.

2. By comparing the case (g) with (f) and (e), we found that the length of CNT is of crucial importance in enhancing the thermal property of CNT-based composites. Increasing the lengths of CNTs is the most effective way to increase the heat conductivity of the composite.

3. The best results are obtained from case (h), which gives the highest values for both the equivalent heat conductivity and the ratio $\kappa/r$, where the conductivity is close to that of metals. With longer CNTs, it is possible to make a CNT-based composite with the heat conductivity equivalent to or higher than that of metals.

## References

1. Endo M., Kim Y.A., Hayashi T., Nishimura K., Matushita T., Miyashita K., Dresselhaus M.S., Vapor-grown carbon fibers: Basic properties and their battery applications, *Carbon*, **39** (2001), pp. 1287-1297.

2. Endo M., Kim Y.A., Nishimura K., Matushita T., Hayashi T., From vapor-grown carbon fibers (VGCFs) to carbon nanotubes. In Carbon filaments and Nanotubes: common origins, Differing Applications, Eds. Biro L. P., Bernardo C.A., Tibbetts G.G. and Lambin Ph., Kluwer *Academic Publishers, NATO Science Series E: Applied Sciences*, **372**(2001), pp. 51-61.

3. Qian D., Dickey E.C., Andrews R., Rantell T., Load transfer and deformation mechanisms in carbon CNT polystyrene composites. *Applied Physics Letters*, **76**(2000), pp. 2868–2870.

4. Biercuk M.J., Llaguno M.C., Radosavljevic M., Hyun J.K., Johnson A.T., Fischer J.E., Carbon nanotube composites for thermal management, *Applied Physics Letters*, **80**, No. 15 (2002), pp. 2767–2769.

5. Liu Y.J., Chen X.L., Evaluations of the effective material properties of carbon CNT-based composites using a nanoscale representative volume element. *Mechanics of Materials*, **35**(2003), pp. 69 -81.

6. Liu Y.J., Nishimura N., Otani Y., Large-scale modeling of carbon-nanotube composites by a fast multipole boundary element method, *Computational Materials Science*. **34**(2005), pp. 173–187.

7. Zhang J.M., Yao Z.H., Li H., A hybrid boundary node method. *Int. J. Numer. Meth. Engng.*, **53**(2002), pp. 751-763.

8. Zhang J.M., Tanaka Masa., Matsumoto T., Meshless analysis of potential problems in three dimensions with the hybrid boundary node method, *Int. J. Numer. Meth. Engng.*, **59** (2004), pp. 1147-1160.

9. Zhang J.M., Tanaka Masa., Matsumoto T., Guzik A., Heat conduction analysis in bodies containing thin-walled structures by means of HdBNM with an application to CNT-based composites, *JSME International Journal Series A: Solid Mechanics and Material Engineering*, **47** (2004), pp. 181-188.

10. Tanaka Masa., Zhang J.M., Matsumoto T., Multi-domain HdBNM for prediction of thermal properties of CNT composites, In: Honma T. and Tanaka Masa. (eds.), *Proceedings of the First Asia-Pacific International Conference on Computational Methods in Engineering* (ICOME 2003, Sapporo, Japan), 2003, pp. 3-12.

11. Zhang J.M., Tanaka Masa., Matsumoto T., A simplified approach for heat conduction analysis of CNT-based nano-composites, *Comput. Methods Appl. Mech. Engrg.*, **193** (2004), pp.5597-5609.

12. Rokhlin V., Rapid solution of integral equations of classical potential theory, *J. Comput. Phys.*, **60** (1985), pp. 187-207.

13. Greengard L., Rokhlin V., A fast algorithm for particles simulations, *J. Comput. Phys.*, **73** (1987), pp. 325-348.

14. Yoshida K., Nishimura N., Kobayashi S., Application of fast multipole Galerkin boundary integral equation method to elastostatic crack problems in 3D, *Int. J. Num. Meth. Eng.*, **50** (2001), pp. 525-547.

15. Nishida T., Hayami K., Application of the fast multipole method to the 3D BEM analysis of electron guns, In: M. Marchettia, C.A. Brebbia, M.H. Aliabadi, ed., *Boundary Elements XIX* (Computational Mechanics Publications, 1997), pp. 613–622.

16. Zhang J.M., Tanaka Masa., Endo M., The hybrid boundary node method accelerated by fast multipole method for 3D potential problems, *Int. J. Num. Meth. Eng.*, **63** (2005), pp. 660-680.

17. Liu Y.J., Nishimura N., Otani Y., Takahashi T., Chen X. L., Munakata H., A Fast Boundary Element Method for the Analysis of Fiber-Reinforced Composites Based on a Rigid-Inclusion Model, *Journal of Applied Mechanics*, **72** (2005), pp. 115-128.

18. Liu Y.J., Rudolphi T.J., New identities for fundamental solutions and their applications to non-singular boundary element formulations, *Computational Mechanics*, **24** (1999), pp. 286-292.